Available online at www.sciencedirect.com
ScienceDirect
Journal of Sound and Vibration 318 (2008) 296–312
JOURNAL OF SOUND AND VIBRATION
www.elsevier.com/locate/jsvi

Time domain contact model for tyre/road interaction including nonlinear contact stiffness due to small-scale roughness

P.B.U. Andersson*, W. Kropp

Division of Applied Acoustics, Chalmers University of Technology, SE-412 96 Göteborg, Sweden

Received 30 October 2007; received in revised form 27 March 2008; accepted 8 April 2008
Handling Editor: C.L. Morfey
Available online 29 May 2008

Abstract

Rolling resistance, traction, wear, excitation of vibrations, and noise generation are all attributes to consider in optimisation of the interaction between automotive tyres and wearing courses of roads. The key to understand and describe the interaction is to include a wide range of length scales in the description of the contact geometry. This means including scales on the order of micrometres that have been neglected in previous tyre/road interaction models. A time domain contact model for the tyre/road interaction that includes interfacial details is presented. The contact geometry is discretised into multiple elements forming pairs of matching points. The dynamic response of the tyre is calculated by convolving the contact forces with pre-calculated Green's functions. The smaller-length scales are included by using constitutive interfacial relations, i.e. by using nonlinear contact springs, for each pair of contact elements. The method is presented for normal (out-of-plane) contact and a method for assessing the stiffness of the nonlinear springs based on detailed geometry and elastic data of the tread is suggested. The governing equations of the nonlinear contact problem are solved with the Newton–Raphson iterative scheme. Relations between force, indentation, and contact stiffness are calculated for a single tread block in contact with a road surface. The calculated results have the same character as results from measurements found in literature. Comparison to traditional contact formulations shows that the effect of the small-scale roughness is large; the contact stiffness is only up to half of the stiffness that would result if contact is made over the whole element directly to the bulk of the tread. It is concluded that the suggested contact formulation is a suitable model to include more details of the contact interface. Further, the presented result for the tread block in contact with the road is a suitable input for a global tyre/road interaction model that is also based on the presented contact formulation.

1. Introduction

There is a steady increase of the road traffic volume. The average annual growth rates in the European Union between 1995 and 2004 have been 1.9% for passenger transport (passenger-kilometres) and 2.8% for freight transport (tonne-kilometres) [1]. Noise generation, rolling resistance, wear, and grip are all determined by the interaction process between the automotive vehicle tyre and the road. The first three attributes affect directly the environment.

*Corresponding author. Tel.: +46 31 772 2202; fax: +46 31 772 2212.
E-mail address: patrik.andersson@chalmers.se (P.B.U. Andersson).

0022-460X/$ - see front matter © 2008 Elsevier Ltd. All rights reserved.
doi:10.1016/j.jsv.2008.04.013

Tyre/road noise is dominating at speeds above 40 km/h for passenger cars and above 70 km/h for lorries [2]. Road traffic noise causes physical and mental health effects, sleep disturbance, and annoyance [3]. As an example, about 70% of the EU population is exposed to road traffic noise with $L_{eq,24\,h}$ (A-weighted equivalent sound pressure level during 24 h) exceeding 55 dB A [4], where a level below 55 dB A is the long term goal for an acceptable sound environment [5].

Rolling resistance is related to energy consumption of the vehicle, which in turn is related to the exhaust gas emissions, such as CO_2, from the engine. Calculations based on the New European Driving Cycle indicates that a 33% decrease in rolling resistance gives about 10% decrease in fuel consumption for middle-class passenger cars [6]. Wear of the tyre and road surfaces will cause emissions of particles into the environment and limit the technical lifetime of both structures. The effect on the environment is under debate, but during its life a tyre loses about 10% of its total mass and 30–50% of the tread mass; hundred thousands of tonnes of tyre and road aggregate are lost each year around the world. This attribute is directly linked to the stresses, strains, and slippage in the tyre/road interface. Traction and breaking performance, which is of outermost importance for safety, is also given by the properties at the very interface.

There is an interest in a deepened understanding of the physics of the interaction. A step in this direction is to closely investigate the influence of the wide range of the length-scales in the tyre/road contact. Tyre/road interaction and noise models have traditionally neglected the smaller length scales and their influence on the interaction behaviour. However, as will be demonstrated in this work through numerical simulations, the smaller length scales have a substantial influence on, for instance, the apparent contact stiffness.

In the following an approach for incorporating length-scales smaller than element size chosen for discretisation of the contact problem is presented. The concept of an interfacial layer, sometimes referred to as a third body approach, between the mating objects is used. The main criticism to the approach is that it is generally hard to determine the properties of the interfacial layer in a unique way. Nevertheless, an interfacial layer is, if correctly incorporated, definitely a better approximation of the physical reality, than the traditional approach stating either no contact or full contact at each pairs of contact elements.

This paper presents first an overview of tyre/road interaction and existing tyre/road contact models. Then it presents details of how to efficiently model tyre/road interaction in the time domain in general and how to include an interfacial layer. A method to determine unique constitutive relations in the interfacial layer determined from detailed scans of surface geometry is suggested. Calculated results are finally presented for tread blocks in contact with a road surface from which general conclusions are made.

1.1. Tyre/road interaction

The interaction problem between the tyre and road in rolling conditions is a challenging problem. Its complexity is due to

- the large dimensions of the contact (10–20 cm) relative to the important wavelengths on the tyre structure,
- the time-varying size of the contact area giving a nonlinear contact,
- the wide range of length-scales in the contact geometry causing nonlinear contact stiffness,
- the presence of friction and adhesion forces at the interface leading to stick-slip and stick-snap processes, respectively, and
- the frequency-, temperature-, and strain-dependent material properties of the tyre structure.

The large dimension of the contact is handled by using a spatial discretisation of the contact geometry and a multi-point contact model. The time-varying size of the contact requires that the contact formulation is made in the time domain. The wide range of length-scales is treated in the present paper while the stick-slip and stick-snap behaviour and its modelling is planed to be presented in other publications. Pre-calculated receptance Green's functions of the tyre structure serve as input to the contact model presented in the following. Basically any linear model that includes the deformation of the tread layer and provides results up to at least 3 kHz would suit directly into this contact formulation (e.g. models based on the elastic field equations [7] or waveguide finite element models [8,9]). Models based on linear theory for the interacting bodies and a nonlinear contact formulation have shown to perform well: (i) calculated velocities of material

points following the rotating tyre compared with measured data using accelerometres in grooves of a tyre rolling on a test drum [10] and (ii) the vibrations of the tyre result in radiated noise, where calculated and measured sound pressure levels of pass-by noise have a good agreement as long as the surface has relatively rough texture [11].

1.2. Tyre/road interaction models

This section gives an overview of models considering the nonlinear contact between the tyre and road. Linear contact models are not treated (i.e. models formulated in the frequency domain and the issue of contact filters).

Two main methods are generally used to numerically solve nonlinear contact problems based on spatial discretisation: the method of Lagrange multipliers and the penalty method. The contact problem may be formulated such that the motion is constrained by inequalities: a condition on the magnitude of the contact force, a geometrical no-penetration condition at the matching points, and a condition of zero contact force when the matching points are separated. Then the method of Lagrange multipliers yields a mathematical formulation and a solution where the conditions are exactly fulfilled. An alternative is to use the penalty method, where stiff penalty springs are added between each pair of matching points. The solution is approximate since penetration occurs and the penetration depth is influenced by the stiffness of the penalty springs. The penalty method is the most widely used method because only the displacement variables enter the equation system. In the Lagrange multiplier method, in addition, the contact forces are present in the system of equations.

Notice that even though the use of Lagrange multipliers yields an exact solution of the formulated problem, the boundary conditions in the method are unrealistic when stating either no contact or full contact at each element. The small length-scale roughness always gives a smoother transition with partial contact in practical applications. The area of real contact, and hence the contact stiffness, increase with load, and there is a nonlinear apparent stiffness between the elements in contact. In a way, the lower apparent stiffness is partly and very approximately reflected by the linear penalty springs in the penalty method. Hence, even though the penalty method yields an approximate solution of the idealised contact problem, the penalty springs includes a somewhat more realistic boundary condition compared with the method of Lagrange multipliers.

Tyres have historically been modelled by beam, ring, and plate models or finite element models with shell elements neglecting deformations of the outermost surface of the tread, only considering displacements and rotations of the neutral line/layer of the structure; the deformation of the tread cap layer relative to the neutral layer is not included and wave propagation in the tread is neglected in these tyre models. The tread has instead been included in the contact models by using a Winkler bedding [12–15] (a layer of uncoupled springs) or an elastic half-space [10]. The Winkler bedding is identical to the standard penalty method except for a considerably lower spring stiffness related to the physical stiffness of the tread. The approximation of no coupling between the springs, which neglects the coupling of the displacements within the tread, is a drawback. The use of elastic half-spaces is a standard approach for (quasi-) static problems in contact mechanics and is preferably solved with an iterative active set strategy [16]. The use of a half-space considers the coupling between points on the half-space, but it is purely elastic without inertia or losses and reacts directly everywhere for any applied load; i.e. the wave speed is infinite in the half-space, which often makes it unsuitable for dynamic problems. It is generally hard to find the single-valued stiffness of the bedding springs or elastic half-space from information about the frequency-dependent Young's modulus and loss factor of the tread material; the spring stiffness or Young's modulus in the models have been updated until correct static deformation is found [13,17].

Later tyre models include the tread layer and give the response of the outermost surface of the tyre (e.g. [7–9,18]), and the Winkler bedding or elastic half-space approaches become redundant in their role of modelling the tread layer. The contact between a tyre including the tread and the road surface can be solved with aid of the method of Lagrange multipliers; e.g. the tyre/road contact model implemented by Larsson [19]. However, the modelling approach gives generally a contact that is so stiff that contact resonances are easily encountered on smoother surfaces. The reason is that the roughness within the elements is neglected and the idealised geometry has the result that the matching points in a pair are either not in contact or in full contact;

there are no states in between. Hence, the contact stiffness will be that of the bulk of the tyre structure. As stated before, in reality the roughness of the surface gives a smooth increase in the area of real contact for increasing load, and the partial contact within the element gives a lower apparent contact stiffness at each pair of elements.

Even though it is not commented upon in the literature, it must be that the small-scale roughness was partly and approximately included in the previous contact models through the model updating of the stiffness of the Winkler bedding springs or the elastic half-space; the stiffness of the springs or half-space is always chosen lower than the one given by the bulk stiffness of the tread.

1.3. Discretisation of contact geometry

The first step in a numerical model of the contact problem is to make a spatial discretisation of the contact geometry. The geometry of the road surface is commonly represented in a three-dimensional coordinate system $(x_i, y_i, z_i(x_i, y_i))$ or along a profile $(x_i, z_i(x_i))$, and is measured with a laser device or a profile meter. The coordinates x_i and y_i are in the plane of the road surface and z_i is the height of the surface normal to this reference plane, while i is a index ranging over all discrete points where coordinates are given. There is generally a trade-off between scanned area or profile length and resolution. Typically, a resolution down to the micrometre length-scale is only available over areas of some centimetres or decimetres squared (Fig. 1), while profiles corresponding to several revolutions of the tyre have a resolution on the order of millimetres.

It is not feasible to use the detailed surface geometry directly in contact models due to the vast number of samples leading to a very high computational cost. The surfaces are instead divided into larger discrete elements and the geometry is represented with one height or several heights for each contact element while the details on shorter lengths are neglected (Fig. 2). A re-sampling technique must be employed if the resolution of the geometry data is different from the spatial discretisation, e.g. using the mean or maximum height within the element, or a low-pass filtering and re-sampling.

The discretisation gives an approximation of the geometry that neglects the roughness on length-scales smaller than the dimensions of the element; see how the geometry within the element is lost in Figs. 1 and 2. Road surfaces have roughness on a wide range of length-scales all the way down to the micro- and nano-metre length-scales. Methods must be employed to include the small-scale roughness within the elements after the discretisation is made.

1.4. Nonlinear constitutive contact relations

A general way to include roughness within elements in a contact model is to use constitutive contact equations for force/pressure–displacement relations within the element area. A constitutive equation can be formulated as a relation between the normal apparent pressure, p_m, and the distance between the surfaces, d_m, at element m,

$$p_m = f(d_m) \quad \text{or} \quad d_m = h(p_m). \tag{1}$$

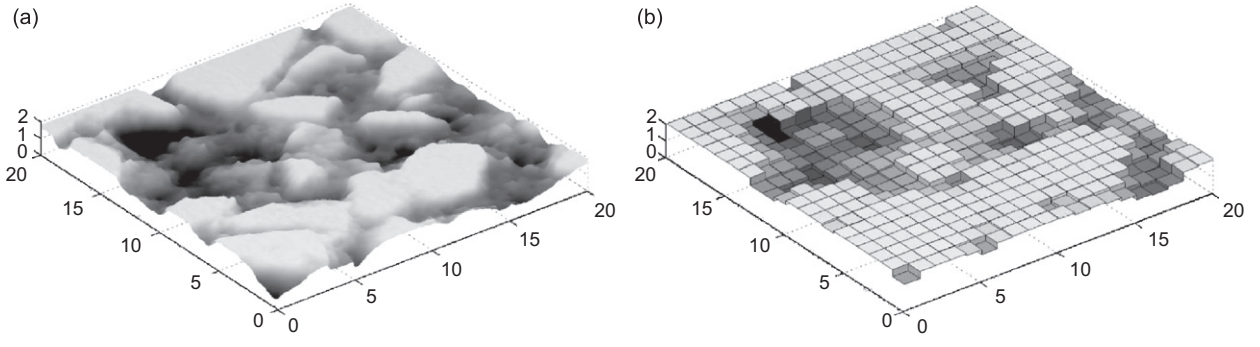

Fig. 1. (a) Detailed scan of road surface geometry and (b) a sampled version of the same geometry. Distances in mm.

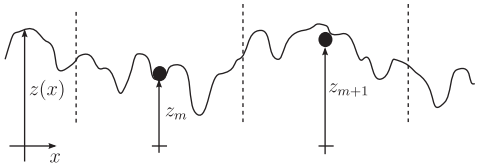

Fig. 2. The geometry of a profile $z(x)$ (solid line) is divided into elements (element m and $m+1$ is between the vertical dashed lines) and the matching points is represented with heights z_m and z_{m+1} (dots).

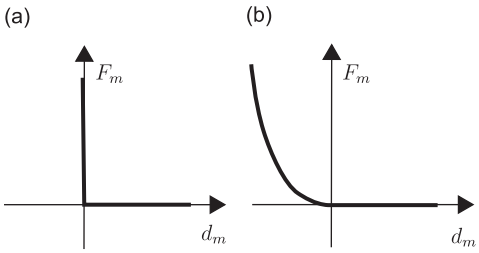

Fig. 3. Contact force versus distance between the matching points. Formulation with (a) Lagrange multipliers and with (b) an interfacial law.

The functions $f(\cdot)$ and $h(\cdot)$ may be determined either from models based on a statistical description of the surface geometry, curve-fitting to measured data, or from numerical contact models based on spatial discretisation with fine resolution. The relations may alternatively be given in terms of the total force acting over the element, F_m, and the distance between the matching points, d_m, by assuming a uniformly distributed apparent pressure over the element with area A_m,

$$F_m = A_m f(d_m) \quad \text{or} \quad d_m = h(F_m/A_m). \tag{2}$$

These interfacial laws give a smoother contact relation compared to the standard method of Lagrange multipliers (Fig. 3).

The behaviour of contact between rough surfaces may be described by various models based on different approaches. E.g. a model consisting of a statistical model of the surface geometry and a mechanical model of the contact at individual junctions [20], power laws based on experimental investigations [21], or statistical surface models [22]. A third-body approach with a continuum layer with nonlinear stiffness added between the bodies in contact was used in Ref. [23]. Generally, the models have several parameters that have to be determined by model updating, either from statistical data of the surface geometry or directly from experimental investigations of the contact problem at hand. The method presented in this paper, on the other hand, uses directly detailed scans of the geometry to find the interfacial laws and they are given individually for each pair of contact elements.

The relations within the elements are commonly assumed to be independent of the states at the other elements, in order to obtain a contact model that is sufficiently fast. Note that the elements are still coupled through the bulk of the body. A nonlinear uncoupled spring between each pair of contact elements is the physical equivalent of a local constitutive equation. Most presented interfacial laws describe in fact the behaviour of a nonlinear spring. The assumption of no inertia may be justified as the modelled surface layer is very thin and exhibits mainly a spring character. Coupling between the springs of adjacent elements can be neglected as an approximation, since the rough surface makes a discontinuous contact, and hence the coupling occurs mainly through the bulk.

2. Contact model

The contact model proposed is presented first for a single pair of contact elements for simplicity, and is thereafter extended to its discrete version and to multiple contact elements. Further, the model is only

presented for non-rotation objects, but the extension to consider a rotating tyre is straightforward; the road geometry are made rotating around the tyre using a reference frame fixed to the tyre.

The contact approach can generally be applied to contact between other objects than tyre and road, but it must be high-lighted that the dynamic response of a tyre have benefits due to the relatively low stiffness of the soft tread and the high-energy dissipation in the structure. Problems with instability in the contact algorithm may arise if structures with low-energy dissipation are considered. This problem can often be treated by an increase of the sampling frequency and length of the Green functions used in the algorithm—in theory but not always in practice due to the increased computational cost.

2.1. Spatial discretisation

In the following it is assumed that the mesh on both the tyre and the road are regular and that they coincide in such a way that a pair of elements that potentially makes contact is formed. The reason for making this restriction is two-fold: (i) it is the way the contact algorithm is presently implemented and for which the results are presented in Section 4 and (ii) it simplifies the presentation of the approach, which rather is about including the interfacial layer than the discretisation of the bulks of the objects in contact. In general, non-matching meshes may be used and techniques for this is treated in standard textbooks (e.g. Ref. [24] where the interested reader may find further references). A pair of elements potentially in contact has an associated pair of matching points. The matching point is located at the centre of each element and its height is given by the outermost coordinate within each element. Having zero distance between the elements exactly when the first contact is made is suitable in conjunction with the interfacial laws presented below.

2.2. Green's functions

The displacement response of a linear dynamic system may be calculated by convolving the external forces acting on the system with Green's functions of the system. The Green function $g(t)$ is generally the solution to

$$\mathbf{L}g(t) = \delta(t), \tag{3}$$

where $\mathbf{L}$ is a linear self-adjoint differential operator and $\delta(\cdot)$ the Dirac delta pulse. The unknown function $u(t)$, which is a solution to

$$\mathbf{L}u(t) = F(t) \tag{4}$$

is then given by

$$u(t) = F(t) * g(t) = \int F(\tau)g(t-\tau)\,\mathrm{d}t. \tag{5}$$

The function $F(t)$ describes in general an external excitation and in specific an external (contact) force for the contact model presented. The right-hand side of Eq. (5) is called a convolution between $F(t)$ and $g(t)$. To be strict, if there are boundary conditions then both $g(t)$ and $u(t)$ must fulfil them.

In the contact model, the Green function is used to describe the displacement of the matching point in one element due to a pulse in time that is uniformly distributed in space over the same or an other element. In other words, the Green function is the solution of the differential equation describing the dynamic response of the tyre structure when the external excitation term is

$$\frac{\delta(t)}{A_m}[H(x-x_1) - H(x-x_2)][(H(y-y_1) - H(y-y_2))], \tag{6}$$

where $A_m = (x_2 - x_1)(y_2 - y_1)$ is the area of the element and $H(\cdot)$ the Heaviside step function. For simplicity, it is assumed that the element is rectangular and oriented in the xy-plane so that its area is described by the coordinates (x, y) for $x_1 \leqslant x \leqslant x_2$ and $y_1 \leqslant y \leqslant y_2$. Note that integrating Eq. (6) over space yields the Dirac delta pulse. Hence, the displacement of the matching point can be found by convolving the total force acting on the element with the calculated Green's function. In the following all equations are formulated in terms of this force instead of the underlying pressure distribution. Note that the Green function has unit m/N s.

The main strength of a contact model with the convolution technique is that it requires a relatively low computational cost. The Green functions can be calculated beforehand by any suitable tyre response model. It is only the displacements of the outer boundary of the tyre that enter the equations to be solved; the displacements within the tyre do not have to be considered. This approach has been applied to various contact problems, e.g. the string/bow contact of a musical instrument [25], beam/rod contact modelling valves [26,27], wheel/rail contact [28], and the tyre/road contact [13,19,17].

2.3. Contact formulation including nonlinear contact springs

The same convolution technique is used here to calculate the displacement field on the bodies in contact, but the contact model is extended to include constitutive contact relations. The model is presented in a general way by adding nonlinear springs between each pair of matching points. The relations between force and displacement at the element can be modelled by choosing an appropriate stiffness function of the spring. The model is first presented for a single pair of matching points for clarity and is later extended to multipoint contact.

Consider two bodies with rough surfaces making contact in a single contact zone (Fig. 4). This zone can be modelled with a pair of contact elements, with the position of each represented by a single matching point. Fig. 5 shows the general idea of the modelling approach where a nonlinear spring is added between the pair of matching points. The distance z_1 gives the position of the matching point at the surface of body 1 when the system is at rest, i.e. when no forces act on the body, and z_2 is the corresponding position of the matching point on body 2. The distance is given relative to a reference plane perpendicular to the direction of the contact. The distances $w_1(t)$ and $w_2(t)$ are the displacements of the matching points of body 1 and body 2, respectively, due to deformations of the bulk of the objects, but not including the small-scale deformation within the element. The distance between the two matching points is $d(t)$ and, hence, negative $d(t)$ means that the surfaces are indenting each other on smaller length-scales. The compression of the spring, $\zeta(t)$, is given by

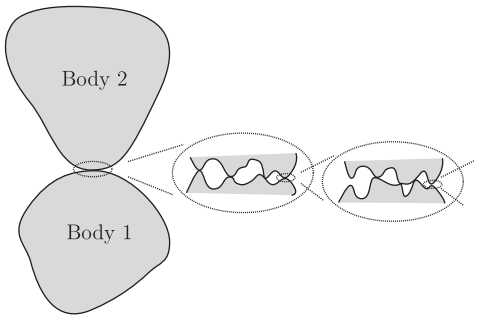

Fig. 4. Two bodies with rough surfaces in contact.

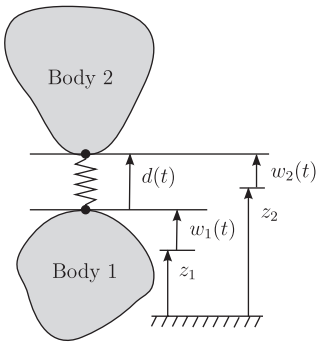

Fig. 5. Geometry and modelling approach of the problem.

the negative separation distance:

$$\zeta(t) = -d(t) = -z_2 - w_2(t) + z_1(t) + w_1(t). \tag{7}$$

Hence, the compression increases when the indentation is increasing.

The displacement of the matching point on body 2, $w_2(t)$, is calculated by convolving the contact force, $F(t)$, with the displacement Green's function of the system, $g(t)$,

$$w_2(t) = F(t) * g(t), \tag{8}$$

just as discussed above. The same kind of relation holds generally for body 1, but in the following this body will be regarded as rigid, i.e. having infinite impedance, for simplicity. The reason is also that this is a clever assumption when modelling the response of the road surface as discussed below. In this case the displacement of the matching point due to deformation is zero,

$$w_1(t) = 0. \tag{9}$$

The constitutive relation between the force $F(t)$ and the compression of the spring $\zeta(t)$ is generally described by a function $f(\cdot)$,

$$F(t) = f(\zeta(t)), \tag{10}$$

as discussed above. This function may include nonlinearities due to the surface roughness and allow for negative forces due to adhesion forces over the interface. Returning to the model of a spring with nonlinear stiffness, the stiffness is given by the derivative of the function,

$$k(\zeta(t)) = \frac{\mathrm{d}f(\zeta(t))}{\mathrm{d}\zeta(t)}. \tag{11}$$

The relation between the spring compression and the force may be formulated by using this spring stiffness according to

$$F(t) = \int_{-\infty}^{\zeta(t)} k(x)\,\mathrm{d}x. \tag{12}$$

If no asperities are making contact when the surfaces are separated by more than a given distance d^0, and hence the spring force is zero, then the lower integration limit can be set to $\zeta^0 = -d^0$. To summarise, Eqs. (7)–(9) and (12) are the governing equations of the problem. The formulation is similar to the standard penalty method but with a nonlinear penalty function, if one regards the spring as the penalty function.

2.4. Time discretisation of the contact problem

The system described by Eqs. (7)–(9) and (12) can generally not be solved analytically, and numerical methods must be employed. Time discretisation is made by low-pass filtering and resampling the signals with a given sampling frequency f_s (constant time step $\Delta t = 1/f_s$). Note that the notations $g(1)$, $g(N)$, $g(N-n)$, etc. used in the following does not mean the continuous function $g(t)$ evaluated at time 1, N, or $N-n$. It means the function $g(t)$ low-pass filtered and its 1st, Nth, or $(N-n)$th sample. This holds for all the functions below except $k(x)$.

Eq. (8) yields for time step N

$$w_2(N) = F(N)g(1)\Delta t + w_2^{\mathrm{old}}(N), \tag{13}$$

where the convolution integral is taken over sampled signals, and

$$w_2^{\mathrm{old}}(N) = \sum_{n=1}^{N-1} F(n)g(N-n+1)\Delta t \tag{14}$$

is the displacement of the matching point due to forces acting at previous times. Thus, this part is already evaluated in the previous time step. Eq. (12) gives

$$F(N) = \int_{-\infty}^{\zeta(N)} k(x)\,\mathrm{d}x = F(N-1) + \int_{\zeta(N-1)}^{\zeta(N)} k(x)\,\mathrm{d}x, \tag{15}$$

where $F(N-1)$ is the force and $\zeta(N-1)$ the compression of the spring in the previous time step, which are known at the present time step. The geometrical condition is written as

$$\zeta(N) = -d(N) = -z_2 - w_2(N) + z_1, \tag{16}$$

when $w_1(n)$ is assumed to be zero for all N.

This is a nonlinear equation system when $k(\cdot)$ is non-constant. The Newton–Raphson method is applied to solve the system. The equations are combined and written on the form $f(x) = 0$ where $f(\cdot)$ is a function given by the equation system combined to a single equation and x the unknown argument. The solution is found by using the iterative scheme,

$$x^{\alpha+1} = x^{\alpha} - \frac{f(x^{\alpha})}{f'(x^{\alpha})}. \tag{17}$$

Eqs. (16) and (13) yield

$$f(\zeta(N)) = \zeta(N) + z_2 + w_2(N) - z_1 = 0, \tag{18}$$

$$f(\zeta(N)) = \zeta(N) + F(N)g(1)\Delta t + w_2^{\mathrm{old}}(N) + z_1 - z_2 = 0. \tag{19}$$

Eq. (15) is finally used to yield

$$f(\zeta(N)) = \zeta(N) + \left(F(N-1) + \int_{\zeta(N-1)}^{\zeta(N)} k(x)\,\mathrm{d}x\right) g(1)\Delta t + w_2^{\mathrm{old}}(N) + z_1 - z_2 = 0, \tag{20}$$

where $\zeta(N)$ is the unknown variable. The derivative of $f(\zeta(N))$ is

$$\frac{\mathrm{d}f(\zeta(N))}{\mathrm{d}\zeta(N)} = 1 + k(\zeta(N))g(1)\Delta t. \tag{21}$$

Hence, the iterative scheme of the Newton–Raphson method reads

$$\zeta^{\alpha+1}(N) = \zeta^{\alpha}(N) - \frac{f(\zeta^{\alpha}(N))}{1 + k(\zeta^{\alpha}(N)} \tag{22}$$

with $f(\zeta^{\alpha}(N))$ given by Eq. (20).

2.5. Multiple contact elements

There are in general multiple pairs of contact elements and an equation system that describes the contact problem. The Newton–Raphson method for a system with M equations and M unknowns is employed. The equations are rewritten in the form

$$f_e(x_1, \ldots, x_M) = 0 \quad \text{for } e = 1, \ldots, M \tag{23}$$

or with compact notation as

$$\mathbf{f}(\mathbf{x}) = \mathbf{0}. \tag{24}$$

The iteration $\mathbf{x}^{\alpha} \to \mathbf{x}^{\alpha+1}$ is made by solving the linear system

$$M(\mathbf{x}^{\alpha})(\mathbf{x}^{\alpha+1} - \mathbf{x}^{\alpha}) + \mathbf{f}(\mathbf{x}^{\alpha}) = 0, \tag{25}$$

where $M(\mathbf{x}) = (\partial f_e/\partial x_m)$ is the functional matrix.

The contact problem described above is extended to multiple pairs of contact elements. The displacement response of the matching point $w_{2,e}(t)$ at contact element e due to the force $F_m(t)$ at element m is given by

$$w_{2,e} = \sum_{m=1}^{M} F_m(t) * g_{m,e}(t) \quad \text{for } e = 1, \ldots, M, \tag{26}$$

where $g_{m,e}(t)$ is the Green function. The spring force at element m is given by

$$F_m(t) = \int_{-\infty}^{\zeta_m(t)} k_m(x)\,\mathrm{d}x \tag{27}$$

and the geometrical condition at the same element is

$$\zeta_m(t) = -z_{2,m} - w_{2,m}(t) + z_{1,m}. \tag{28}$$

Time discretisation, using the same notation as for the single equation case, yields

$$w_{2,e}(N) = \sum_{m=1}^{M} F_m(N) g_{m,e}(1)\Delta t + w_{2,e}^{\mathrm{old}}(N), \tag{29}$$

$$F_m(N) = F_m(N-1) + \int_{\zeta_m(N-1)}^{\zeta_m(N)} k_m(x)\,\mathrm{d}x, \tag{30}$$

$$\zeta_e(N) = -z_{2,e} - w_{2,e}(N) + z_{1,e}. \tag{31}$$

These equations are combined into functions of the form $f_e(\zeta_1(N), \zeta_2(N), \ldots, \zeta_M(N)) = 0$,

$$f_e(\zeta_1(N), \zeta_2(N), \ldots, \zeta_M(N)) = \zeta_e(N) + \sum_{m=1}^{M}\left(F_m(N-1) + \int_{\zeta_m(N-1)}^{\zeta_m(N)} k_m(x)\,\mathrm{d}x\right) g_{e,m}(1)\Delta t + w_{2,e}^{\mathrm{old}}(N) + z_{2,e} - z_{1,e} = 0. \tag{32}$$

The corresponding derivatives in the functional matrix are given by

$$\frac{\partial f_e(\zeta_1(N), \zeta_2(N), \ldots, \zeta_M(N))}{\partial \zeta_m(N)} = \delta_{e,m} + k_m(\zeta_m(N)) g_{e,m}(1)\Delta t, \tag{33}$$

where

$$\delta_{e,m} = \begin{cases} 1 & \text{if } e = m \\ 0 & \text{if } e \neq m. \end{cases}$$

The equations describe a general way of incorporating nonlinear stiffness between the matching points. The functions $k_m(\cdot)$ must be given in order to solve the system. Note that all elements on body 2 are coupled via the first value of the Green function in Eq. (29), but the constitutive *relation* at element m, described by Eq. (30), is independent of the compressions of the springs at adjacent elements.

2.6. Method for estimating the nonlinear stiffness functions

The stiffness functions of the nonlinear springs within each pair of contact elements, arising from the smallest length-scales, are determined from detailed scans of the surface geometry, elastic data of the tread, and a model of a flat circular punch indenting an elastic layer. The approach gives an estimation of a stiffness function that is unique for each pair of contact elements. The very smallest length-scales are still neglected due to the finite resolution of the measurement device when scanning the surface, but including length-scales down to micrometres is definitely a step in the right direction.

There are two fundamental properties that the stiffness functions must have: The interfacial stiffness (i) should start from zero when the first contact is made and be monotonically increasing for increased load/indentation and (ii) should be infinite when complete saturation occurs. The latter case means that the surfaces of the bulks of the interacting objects have direct contact all over the interface and thus the deformation only occurs in the bulks.

A model of a rigid and flat circular punch indenting an elastic layer is used as an approximation to estimate the interfacial stiffness. This is a standard contact problem for which relations between contact pressure, total force, and indentation are available in literature (e.g. Ref. [29]). Assuming that the indentation is made with a flat circular punch will give an overestimation of the stiffness for cases where in reality several disjoint patches

are present to transfer the force. A more detailed model that considers coordinates that forms separated patches can be used and is a natural path for future refinement of the model if needed.

The actual contact geometry has to be translated to a radius of the punch and a thickness of the elastic layer. The roughness is assumed to yield a thin interfacial layer determined by the difference between maximum and minimum height, $z_{\max}$ and $z_{\min}$, of the road surface within the element under consideration. For each element, the area of contact is estimated by considering the area of heights above a given indentation (compression of the spring) ζ,

$$A(\zeta) = \sum_i H(z_i - (z_{\max} - \zeta))\,\mathrm{d}A, \tag{34}$$

where $H(\cdot)$ is the Heaviside step function and $\mathrm{d}A$ the area associated with each surface point (Fig. 6). The estimated area of real contact is used to calculate the equivalent radius of the circular punch

$$r_{\mathrm{eq}}(\zeta) = \sqrt{A(\zeta)/\pi}. \tag{35}$$

The layer thickness is assumed to depend on the indentation ζ as

$$h(\zeta) = (z_{\max} - \zeta) - z_{\min}, \tag{36}$$

where $z_{\min}$ is the lowest height within the present contact element. This choice of layer thickness assures that the interfacial contact stiffness becomes infinite for complete saturation (which in practice never occurs). The relations for the flat circular punch of radius $r_{\mathrm{eq}}(\zeta)$ indenting an elastic layer of thickness $h(\zeta)$ is used to numerically determine the stiffness functions. In practice it is convenient to describe the final stiffness function by a polynomial approximation where a polynomial order of ten have been found suitable. Fig. 7 shows the typical character of the stiffness functions for five different pairs of elements. Note that the stiffness is very close to the stiffness of the elastic half-space approximation at low compressions, where the contact area is small in comparison to the layer thickness. As the compressions increases the effect of the finite layer thickness starts to be more pronounced.

2.7. Discussion about existence and uniqueness

Existence and uniqueness of the solution of the formulated contact problems have not been addressed above. The approximate solution of the Newton–Raphson method converges quadratically to the global minimum if the starting estimate is close enough to the solution. There is a general requirement of the

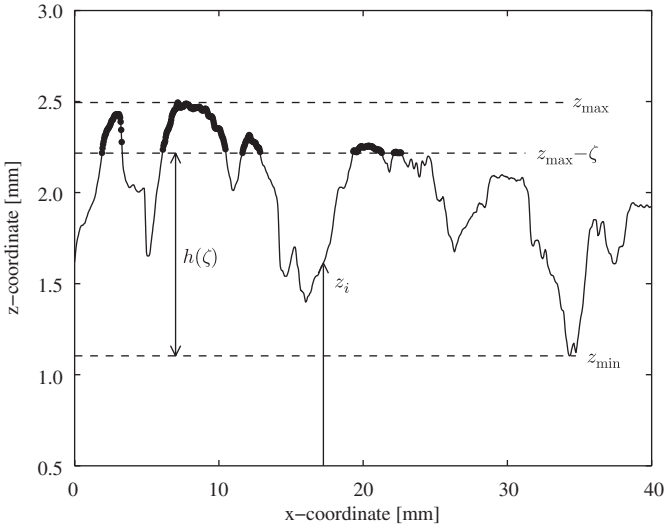

Fig. 6. The detailed surface profile record z_i and the maximum and minimum heights $z_{\max}$ and $z_{\min}$, the indentation ζ and the layer thickness $h(\zeta)$.

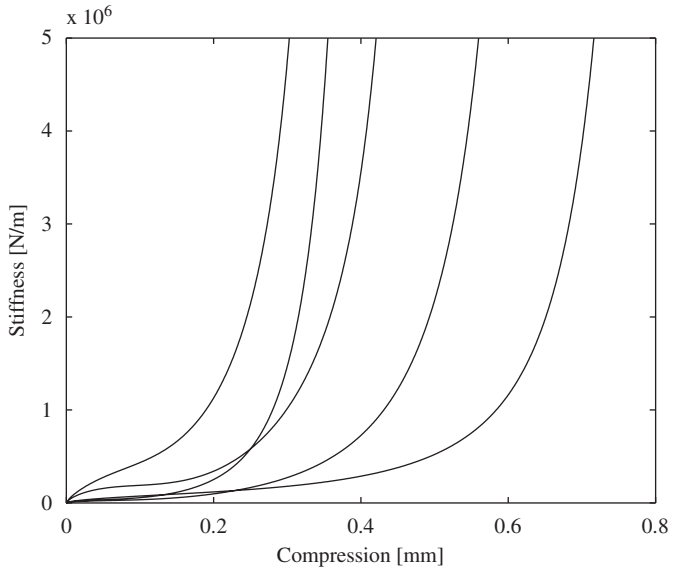

Fig. 7. Five typical stiffness functions.

functions to be regular for convergence, i.e. they should be analytical and differentiable. The requirement of differentiability is clearly seen as the functional matrix used in the iteration contains the derivatives of the functions. Convergence to a unique solution is expected when the stiffness functions are regular and monotonically increasing for increased compression of the spring. However, if adhesion forces are modelled, which has two compressions giving the same force, then the solution is non-unique. Choosing sufficiently small time steps, and a linearisation from the previous contact state as a starting point, generally yields convergence to the solution closest to the previous one.

Note that also contact models including stick-slip motion by using the friction law of Coulomb have generally been loosely founded with respect to convergence; the problems are known to exhibit features such as non-uniqueness and even non-existence. Trial-and-error approaches have been applied, where models giving the expected results have been judged useful. Some effort has been spent on convergence, which can be proven if the friction law is regularised. The problem has also been put in the framework of mathematical programming theory, and convergence have been proved for less strict requirements of differentiability on the functions [30].

3. Simulations

Simulations using the contact model presented above are made for a single tread block in contact with a road surface. The contact is made at various positions of the road sample to investigate the spatial variations of the contact stiffness. The set of Green's functions for the tread is modelled using a numerical model solving the elastic field equations in the frequency/wavenumber domain. It is the model presented in Refs. [7,31] but with boundary conditions for a 1 cm thick tread layer with a rigid backing. The model gives frequency response functions that are transformed to the time domain (by using the technique presented in Ref. [32] to assure causality and the correct static deformation, and to reduce ripples due to the Gibbs phenomenon). The Young modulus of the tread has a real part of 25 MPa at 0 Hz that increases with frequency up to 50 MPa. The imaginary part starts from 0 MPa at 0 Hz and increases with frequency up to 25 MPa at the highest frequencies considered. The resulting Green functions are 256 samples long with a sampling frequency of 51.2 kHz.

The road surface is a scan of a wearing course built according to the standard ISO-10844 [33], which is a test track specification commonly used as a reference case for tyre/road interaction. The smaller length-scales are given in a regular grid with a resolution of 38 μm. The road surface is assumed to have infinite mechanical impedance and the road geometry is simply included in the contact problem through a geometrical boundary

condition, i.e. the road is assumed to be rigid. This is a most common simplification in models of tyre/road contact and is justified in most cases by the large difference in mechanical impedance between the road and tyre structures. It is however not valid for roads with relatively low mechanical impedance, such as roads with specially designed poroelastic wearing courses.

The contact is made over an apparent area of 2 cm × 2 cm and the contact area is divided into 20 × 20 elements as the standard case. The same sampling frequency as is used for the Green functions, i.e. 51.2 kHz, is used in the contact algorithm. The loading is chosen to simulate a (quasi-)static case with a prescribed indentation where the distance $z_2 - z_1$ is decreased in steps of 0.01 μm. The number of time steps used in each indentation step is more than the number of samples of the Green functions to get the static result. The contact problem is in practice solved by using an outer loop with an active set strategy, i.e. an algorithm that in each time step identifies the elements that actually makes contact so that only these elements needs to be considered in the contact problem to be solved. This decreases the computational cost substantially as only part of the pairs of elements actually makes contact for the considered loads.

4. Results and discussion

Selected results from the simulations are presented in the following to highlight the performance of the contact model and to show typical results for a tread block in contact with a road surface.

4.1. Performance of the model

The presented contact modelling including the small-scale roughness gives a considerable smoother and softer contact for a tread block than a standard formulation with Lagrange multipliers (Fig. 8). The standard formulation brutally states either no contact or full contact at each pair of contact elements as shown in Fig. 3a. The difference is also seen as the number of active matching points is increased and the forces decreases compared to the standard formulation. It is clear that the presented formulation shows the softer contact stiffness and the smooth relation between indentation and contact stiffness that follow from fundamentals of contact between objects with rough surfaces and the concept of area of real contact.

Fig. 9 shows the contact stiffness as a function of force for different chosen discretisations corresponding to elements of size 1 mm × 1 mm, 1.1111 mm × 1.1111 mm, 1.25 mm × 1.25 mm, 1.4286 mm × 1.4286 mm, 1.667 mm × 1.667 mm, and 2 mm × 2 mm for one single contact position. Different sizes of the element means that different amount of the geometry is included in the spatial discretisation and in the nonlinear

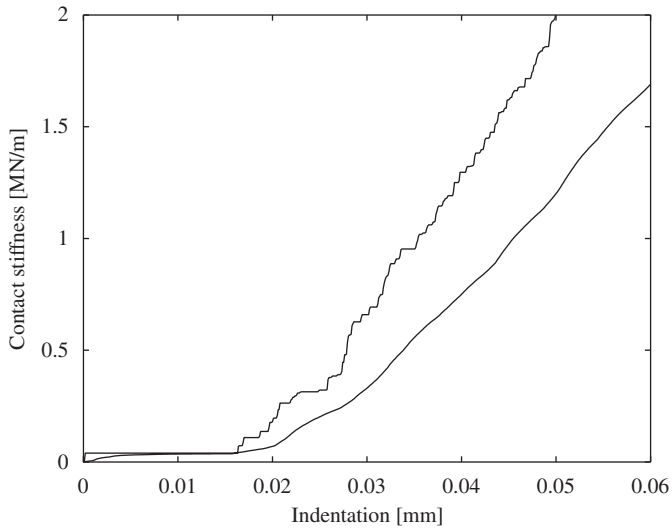

Fig. 8. Contact stiffness as a function of indentation for a tread block in contact with a road surface. Formulation with (thin line) Lagrange multipliers and (thick line) the presented model.

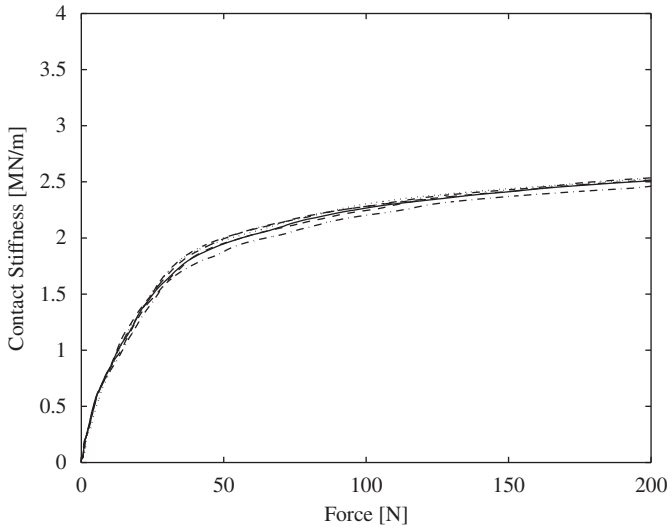

Fig. 9. Contact stiffness as a function of force for discretisation in 20×20 (thick solid line) , 18×18 (thick dashed line), 16×16 (thick dash-dotted line), 14×14 (thick dotted line), 12×12 (thin dash-dotted line), and 10×10 (thin dashed line) elements.

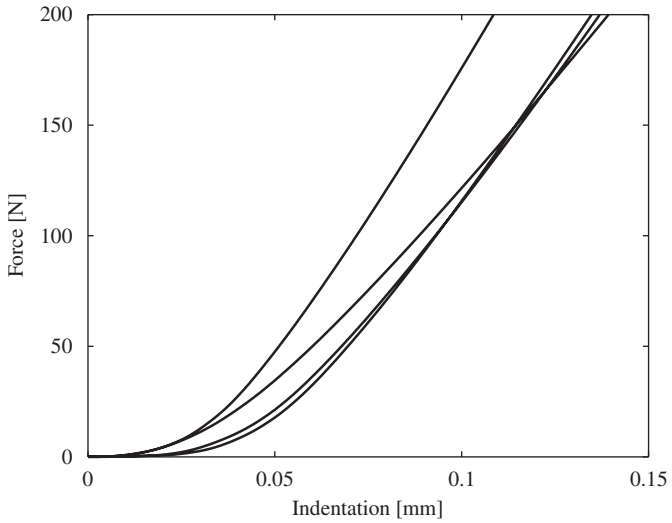

Fig. 10. Force as a function of indentation depth for four different positions on the same wearing course. Position A (solid line), B (dashed line), C (dash-dotted line), and D (dotted line).

contact springs, respectively. It is obvious that the model is rather robust with respect to the chosen discretisation for the presented cases; the difference in contact stiffness at 100 N load is less than 5%. However, the differences in the calculated results starts to be significant when a spatial discretisation with elements larger than 2 mm × 2 mm is used. This is obviously the length-scale where the effect of disjoint patches within the elements starts to be significant. Using a model for the spring stiffnesses that considers the individual patches within each element may be a solution to close this discrepancy.

4.2. Contact stiffness in tyre/road contact

Fig. 10 shows the force–indentation relation for four different positions on the road surface. As expected, there is clearly a nonlinear relation between the total force over the interface and the indentation of the tread into the wearing course. Fig. 11 shows that the corresponding contact stiffness is lower when the first contact is

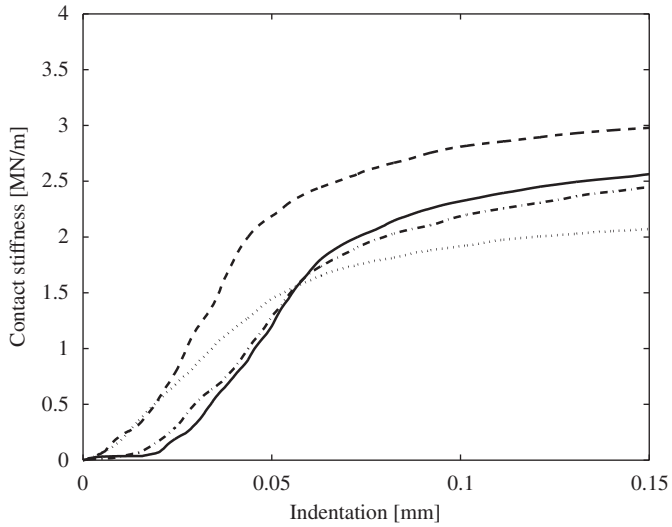

Fig. 11. Contact stiffness as a function of indentation depth for four different positions on the same wearing course. Position A (solid line), B (dashed line), C (dash-dotted line), and D (dotted line).

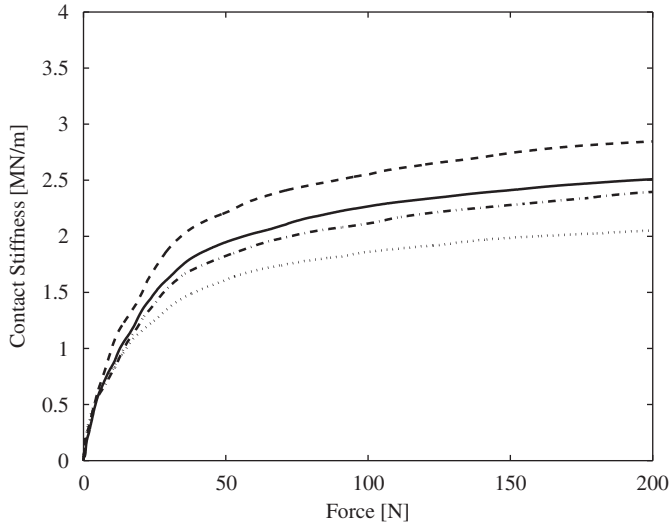

Fig. 12. Contact stiffness as a function of force for four different positions on the same wearing course. Position (solid line) A, (dashed line) B, (dash-dotted line) C, and (dotted line) D.

made and increases as more and more junctions make contact. The contact stiffness varies substantially between the different positions indicating that the spatial variations in the contact geometry are important to consider. The contact stiffness for the case of a perfectly flat contact geometry giving direct contact of the bulks all over the surface would be above 4 MN/m, which is substantially above the one when considering the smaller length-scales in the geometry as the real contact geometry causes only a partial contact. Further, the calculated relations show the same characteristics as the experimental results presented by Kröger and Gäbel [34]. Their measured stiffness is in the order of 10 times lower, but both a different tread and a different road surface was used.

The static load on a tyre is in the order of 4 kN and numerical simulation shows that the dynamic pressure varies ±10% around the static one [17]. A typical contact patch has dimension of 10 cm × 15 cm yielding an average contact pressure of about 300 kPa. Thus the expected force transferred over patch of 2 cm × 2 cm is on the order of 120 N. Fig. 12 shows that the contact stiffness for a block of these dimensions are 1.5–2.5 MN/m

for the expected maximum pressure. However, at the leading edge the load starts from zero and increases as the block enters the contact zone. Thus, the contact stiffness varies substantially not only between different contact geometries but also during the run through the contact.

Using detailed scans of the actual surface geometry is manageable in fundamental studies as the one presented here. However, when studying the complete tyre with multiple revolutions it is not likely that the detailed surface scans would be available over more than an area of the order of 10 cm × 10 cm, i.e. for a single footprint. However it is important to consider both the actual contact stiffness and resulting pressure distribution that clearly vary with position and load, especially when modelling friction forces (stick-slip processes) and adhesion forces (stick-snap processes). It rises the interesting question whether it is applicable to work with simplified stiffness functions or not. Could a stiffness function for each element that is randomly chosen from a smaller set of stiffness functions be used for calculations over several revolutions? The stiffness functions would be pre-calculated for the actual tyre and road under consideration. Or would even a single average stiffness function be applicable? The performance of the tyre/road interaction models based on a Winkler bedding or an elastic half-space (that assumes constant stiffness) used today definitely indicates that simplifications should be applicable when studying the complete rolling tyre on relatively rough surfaces. However, these models definitely fail for smooth tyres on relatively smooth low roughness roads, but future studies in line with the presented may reveal to what degree a more detailed description of the real contact stiffness is needed.

5. Conclusions

The presented contact model is a step towards including more of the interfacial details in the tyre/road contact. The model was demonstrated for normal (out-of-plane) contact only, but it is straightforward to extend the formulation to include also tangential (in-plane) contact using a friction law (which has been implemented by the research group [35]). It is concluded that the model captures more of the actual behaviour at the interface by including also the effect of the smaller length-scales within the elements of the spatial discretisation.

The validity of the presented model has only been indirectly demonstrated. Detailed experimental data for a specific tyre/road combination that include all the necessary components is missing. In fact, validation is generally problematic when including smaller length-scales in view of the advanced experimental devices needed but is planned future work. However, the presented modelling approach is based on previous theories for rough surfaces and natural physical relations, and the results show the characteristic relations following from fundamentals of elastic objects with rough surfaces in contact. The model also follows the characteristics of measured stiffness–indentation relations found in literature (missing details of road geometry and tyre tread material properties). Thus, the presented *approach* to include smaller length-scales has been validated, while future comparisons to experimental results for specific tyre/road combinations may reveal that more (or less) details need to be included in the estimation of the interfacial laws for each pair of contact elements.

The numerical results showed that the effect of the small-scale roughness is substantial. The actual contact stiffness for a block varies between zero and about half of that one given by full contact to the bulk. The presented relations between indentation and force for a single tread block is a suitable input for a global tyre/road interaction model, i.e. a model that includes the complete rotating tyre. The same contact formulation as presented here would be applicable and is planned for future work.

Acknowledgements

The work presented was financially supported by the Swedish Research Council (Project no. 621-2005-5790) and the European Commission (ITARI, FP6-PL-0506437) and (SILENCE, TIP4-CT-2005-516288).

References

[1] ERF (European Union Road Federation), *European Road Statistics 2006*, ⟨http://www.erf.be/images/stat/ERF_stats2006.pdf⟩, 2006.
[2] U. Sandberg, Tyre/Road Noise: Myths and Realities, *Proceedings of InterNoise 2001*, The Hague, The Netherlands, 2001.

[3] B. Berglund, T. Lindvall, Community Noise. Document prepared for the World Health Organization, *Archives of the Centre for Sensory Research* 2 (1995) 1–195.
[4] B. Vincent, J. Lambert, Assessing the quality of urban sound environment: complementarity between noise monitoring system, noise mapping and perception survey, the stakes for the information to the public, *Proceedings of InterNoise 2005*, Rio de Janeiro, Brazil, 2005.
[5] D. Stanners, P. Bordeau, European Environment, Technical Report E97-01, European Environment Agency, 1995.
[6] U. Sandberg, J. Ejsmont, *Tyre/Road Noise Reference Book*, first ed., Informex, SE-59040 Kisa, Sweden, 2002.
[7] K. Larsson, W. Kropp, A high frequency three-dimensional tyre model based on two coupled leastic layers, *Journal of Sound and Vibration* 253 (2002) 889–908.
[8] C.-M. Nilsson, Waveguide Finite Elements Applied on a Car Tyre, Doctoral Thesis, Dept. of Aeronautical and Vehicle Technology, Royal Institute of Technology, Stockholm, Sweden, 2002.
[9] P. Sabiniarz, On the Waveguide Finite Element Method for Modelling Vibrations—General Investigation and Application to a Cartyre, M.Sc. Thesis E04-15, Department of Applied Acoustics, Chalmers University of Technology, Göteborg, Sweden, 2004.
[10] F. Wullens, W. Kropp, A three-dimensional contact model for tyre/road interaction in rolling conditions, *ActaAcustica/Acustica* 90 (2004) 702–711.
[11] W. Kropp, K. Larsson, F. Wullens, P. Andersson, F.-X. Bécot, T. Beckenbauer, *The Modelling of Tyre/Road Noise—A Quasi Three-Dimensional Model*, *Proceedings of InterNoise 2001*, The Hague, The Netherlands, 2001.
[12] K. Johnson, *Contact Mechanics*, ISBN 0-521-34796-3, Cambridge University Press, UK, 1985.
[13] W. Kropp, Ein Modell zur Beschreibung des Rollgeräusches eines Unprofilierten Gürtelreifens auf Rauher Straßenoberfläche, PhD Thesis, Fortschrittberichte VDI, Reihe 11: Schwingungtstechnik, N. 166, 1992.
[14] J.-F. Hamet, P. Klein, Use of a rolling model for the study of the correlation between road texture and tire noise, *Proceedings of InterNoise 2001*, The Hague, The Netherlands, 2001.
[15] E. Gerretsen, E. Schoen, F. van der Eerden, E. Mulder, *Relevant parameters for low-noise tyre designs—and optimisation study*, TNO report HAG-RPT-010163, TNO-TPD, Sound and Vibration Division, Delft, The Netherlands, 2002.
[16] J. Kalker, *Three-dimensional Elastic Bodies in Rolling Contact (Solid Mechanics and its Applications)*, Kluwer Academic Publishers, Dordrecht, 1990.
[17] F. Wullens, Excitation of Tyre Vibrations due to Tyre/Road Interaction, PhD Thesis F04-03, Department of Applied Acoustics, Chalmers University of Technology, Göteborg, Sweden, 2004.
[18] S. Finnveden, C.-M. Nilsson, M. Fraggstedt, Waveguide FEA of the vibration of rolling car tyres, *Proceedings of NOVEM*, Saint-Raphael, France, 2005.
[19] K. Larsson, Modelling of Dynamic Contact. Exemplified on the Tyre/Road Noise, PhD Thesis F02-02, Department of Applied Acoustics, Chalmers University of Technology, Göteborg, Sweden, 2002.
[20] K. Willner, L. Gaul, Contact description by FEM based on interface physics, *Proceedings of COMPLAS 5*, Vol. 1, Barcelona, Spain, 1997, pp. 884–891.
[21] I. Kragelsky, *Friction and Wear—Calculation Methods*, Pergamon Press, Oxford, 1982.
[22] G. Zavarise, P. Wriggers, E. Stein, B. Schrefler, A numerical model for thermomechanical contact based on microscopic interface laws, *Mechanics Research Communications* 19 (1992) 173–182.
[23] U. Sellgren, S. Björklund, S. Andersson, A finite element-based model of normal contact between rough surfaces, *Wear* 254 (2003) 1180–1188.
[24] P. Wriggers, *Computational Contact Mechanics*, ISBN 0-471-49680-4, Wiley, West Sussex, England, 2002.
[25] M. McIntyre, R. Schumacher, J. Woodhouse, On the oscillations of musical instruments, *Journal of the Acoustical Society of America* 74 (1983) 1325–1345.
[26] C. Wang, J. Kim, New analysis method for a thin beam impacting against a stop based on the full continuous model, *Journal of Sound and Vibation* 191 (1996) 809–823.
[27] C. Wang, J. Kim, The dynamic analysis of a thin beam impacting against a stop of general three-dimensional geometry, *Journal of Sound and Vibation* 203 (1997) 237–249.
[28] A. Nordborg, Wheel/rail noise generation due to nonlinear effects and parametric excitation, *Journal of the Acoustical Society of America* 111 (2002) 1772–1781.
[29] F. Yang, Indentation of an incompressible elastic film, *Mechanics of Materials* 30 (1998) 275–286.
[30] P. Christensen, A. Klarbring, J. Pang, N. Strömberg, Formulation and comparison of algorithms for frictional contact problems, *International Journal for Numerical Methods in Engineering* 42 (1998) 145–173.
[31] P. Andersson, K. Larsson, Validation of a high frequency three-dimensional tyre model, *ActaAcustica/Acustica* 91 (2005) 121–131.
[32] P. Andersson, Modelling Interfacial Details in Tyre/Road Contact—Adhesion Forces and Non-linear Contact Stiffness, ISBN 91-7291-652-4, PhD Thesis, Division of Applied Acoustics, Chalmers University of Technology, Göteborg, Sweden, 2005.
[33] ISO 10844, *Acoustics—Specification of Test Tracks for the Purpose of Measuring Noise Emitted by Road Vehicles*, International Organization for Standardization, 1994.
[34] G. Gäbel, M. Kröger, Non-linear contact stiffness in tyre-road interaction, *Paper 118*, *The Sixth European Conference on Noise Control* (*EURONOISE2006*), Tampere, Finland, 2006.
[35] P. Sabiniarz, W. Kropp, A model to evaluate the importance of tangential contact forces for tyre/road noise generation, Acoustics'08, Paris, France, 2008.